Molecular Effects, Speciation, and Competition of Inorganic and Methyl Mercury in the Aquatic Plant *Elodea nuttallii*

Beauvais-Flueck, Rebecca; Slaveykova, Vera; Skyllberg, Ulf; Cosio, Claudia

How to cite

BEAUVAIS-FLUECK, Rebecca et al. Molecular Effects, Speciation, and Competition of Inorganic and Methyl Mercury in the Aquatic Plant *Elodea nuttallii*. In: Environmental Science & Technology, 2018, vol. 52, n° 15, p. 8876–8884. doi: 10.1021/acs.est.8b02124

This publication URL: https://archive-ouverte.unige.ch/unige:107325
Publication DOI: 10.1021/acs.est.8b02124

Molecular effects of inorganic and methyl mercury in single exposure and mixture scenarios in the aquatic plant *Elodea nuttallii*

Rébecca Beauvais-Flück, Vera I. Slaveykova, Claudia Cosio[†]

Department F.-A. Forel for environmental and aquatic sciences, Earth and Environmental Sciences, Faculty of Sciences, University of Geneva, 66, boulevard Carl-Vogt, 1211 Genève 4, Switzerland.

[†]present address: Unité Stress Environnementaux et BIOSurveillance des Milieux Aquatiques UMR-I 02 (SEBIO), Université de Reims Champagne Ardenne, F-51687 Reims, France.

*Corresponding author: claudia.cosio@unige.ch, claudia.cosio@univ-reims.fr

Abstract

Mercury (Hg) accumulation in aquatic food webs remains a hazard worldwide, nonetheless Hg uptake and impact in aquatic plants is poorly understood. We characterized the cellular toxicity pathways of a range of inorganic Hg (IHg) and methyl Hg (MeHg) concentrations (0.01 to 15 $\mu g \cdot L^{-1}$) in the aquatic plant *Elodea nuttallii*. Regulated biological pathways identified by transcriptomic (RNA-sequencing) supported a similar response to IHg and MeHg, both affecting contigs involved in energy metabolism (photosynthesis, sugar metabolism), cell structure (development and cell wall), transport (vacuolar and nutrition), and secondary metabolism (flavonoids). Nevertheless, the number of significantly regulated contigs was higher for MeHg than IHg, including when IHg treatment resulted in higher intracellular concentrations than MeHg. Data thus point to a higher molecular impact of MeHg than IHg. At the organism level, both enzymatic (peroxidases) and non-enzymatic anti-oxidants (anthocyanin) were induced by MeHg treatments, while IHg treatments resulted in a higher proportion of binding in cell walls and decreased chlorophyll content.

The expression of a subset of contigs was further studied in IHg-MeHg mixture scenarios, in presence of copper (Cu) and Suwannee river humic acid to improve environmental realism. We identified a distinct gene expression signature for IHg, MeHg and Cu, further supporting different toxicity modes-of-action of these trace elements. Our data provided thus fundamental knowledge on IHg and MeHg uptake and tolerance mechanisms in a key aquatic primary producer and confirmed the potential of developing an early-warning tool using transcriptomics to assess Hg exposure in environmentally realistic systems.

Keywords: copper, dissolved organic matter, pigment, redox, RNA-sequencing, transcriptomic.

Introduction

Mercury (Hg) is one of the most hazardous metals on Earth, mostly because of the biomagnification of its methylated form (MeHg) in aquatic food webs [1]. Freshwater ecosystems remain currently affected by Hg pollution worldwide, despite past and on-going efforts to reduce anthropogenic emissions of Hg [2]. Aquatic plants have a key ecological role in shallow water ecosystems and are instrumental for Hg transfer to top consumers in food webs [3-6]. For example, *Elodea nuttallii* showed high Hg accumulation from sediments and water column [7, 8]. Hg accumulated in plants can impact their fitness and life cycle. In rice seedlings, Hg exposure inhibited root growth and microarray analysis revealed that inorganic Hg (IHg) affected genes involved in amino acid metabolism and water transport [9]. In *E. nuttallii*, analysis of the transcriptome revealed a strong impact of IHg on energy metabolism and metal homeostasis [10]. In the same line, transcriptomics of *E. nuttallii* exposed to MeHg revealed a significant impact on the expression level of genes involved in energy metabolism and water transport [11]. At the organism level, 24h exposure to 70 $ng \cdot L^{-1}$ IHg affected *E. nuttallii* root growth, while 23 $ng \cdot L^{-1}$ MeHg did not [4]. Histology and proteomics further revealed an increased lignification of cell walls in response to IHg exposure [4]. However, most studies were conducted at high concentrations and in simplified conditions. Moreover, to our knowledge no previous study aimed at comparing uptake and effects of IHg and MeHg on the transcriptome of aquatic plants was performed. Detailed characterization of molecular and cellular mechanisms of toxicity and tolerance mechanisms in aquatic plant in realistic conditions is a prerequisite to understand the fate and the impact of IHg and MeHg in the aquatic environment.

This study aimed first to compare the molecular toxicity pathways triggered by 2h-long exposures to a range of IHg and MeHg concentrations (0.01 to 15 $\mu g \cdot L^{-1}$) in the macrophyte *Elodea nuttallii* using whole transcriptome analysis (RNA-Sequencing; RNA-Seq) and physiological endpoints including pigments content (chlorophyll and anthocyanin) and the activity of anti-oxidative enzymes. Subsequently, we investigated the Hg uptake and expression level of a subset of genes in *E. nuttallii* exposed to mixtures, containing IHg, MeHg, dissolved organic matter (DOM) and copper (Cu) to gain fundamental knowledge on Hg uptake and tolerance mechanisms in a key aquatic primary producer in more realistic exposure scenarios.

Material and Methods

Plant exposure conditions

Elodea nuttallii was harvested in Lake Geneva and grown in aquariums containing 1.2 µm-filtered Lake Geneva water and 5 cm of natural sediment from Lake Geneva. For all treatments, shoots (~10 cm-long without roots) were exposed 2h in 500 mL of an artificial medium (91.0 $mg \cdot L^{-1}$ $CaCl_2.2H_2O$, 43.2 $mg \cdot L^{-1}$ $MgSO_4.7H_2O$, 23.5 $mg \cdot L^{-1}$ $NaHCO_3$, 13.6 $mg \cdot L^{-1}$ KH_2PO_4 and 0.4 $mg \cdot L^{-1}$ NH_4NO_3, pH 6.9 ± 0.1) in controlled conditions (16:8h light:dark, 1000 lux, 20°C).

For experiment 1 (whole transcriptome analysis): Shoots were exposed to 0.015, 0.15 and 15 $\mu g \cdot L^{-1}$ IHg ($Hg(NO_3)_2$ solution, Sigma-Aldrich, Buchs, Switzerland) and 0.01, 0.10, 1 or 10 $\mu g \cdot L^{-1}$ MeHg (MeHgCl solution, Ward Hill, MA, USA). For comparison, in Europe, the current environmental quality standard (EQS) for THg in surface water is 0.07 $\mu g \cdot L^{-1}$. In short, we tested a range of concentrations below and above the EQS.

For experiment 2 (targeted transcriptome analysis): Shoots were exposed to 0.15 and 15 $\mu g \cdot L^{-1}$ IHg, 0.25 $\mu g \cdot L^{-1}$ MeHg, 4 $\mu g \cdot L^{-1}$ Cu ($CuSO_4$ solution, Sigma-Aldrich, Buchs, Switzerland) and the following mixtures, to improve environmental realism: 0.15 $\mu g \cdot L^{-1}$ IHg + 0.25 $\mu g \cdot L^{-1}$ MeHg, 15 $\mu g \cdot L^{-1}$ IHg + 0.25 $\mu g \cdot L^{-1}$ MeHg, 0.15 $\mu g \cdot L^{-1}$ IHg + 4 $\mu g \cdot L^{-1}$ Cu, 70 $\mu g \cdot L^{-1}$ IHg + 4 $\mu g \cdot L^{-1}$ Cu and 0.25 $\mu g \cdot L^{-1}$ MeHg + 17 $\mu g \cdot L^{-1}$ Cu. All these conditions were in addition tested in presence of 1 or 10 $mg \cdot L^{-1}$ Suwanee River humic acid (SRHA; International Humic Substances Society, St. Paul, MN, USA). Thereafter treatments without IHg, MeHg, Cu, SRHA are named *Control*, while treatments with SRHA alone (in the absence of metal) are named *1 $mg \cdot L^{-1}$ SRHA* and *10 $mg \cdot L^{-1}$ SRHA* according to their respective concentration.

Total RNA extraction

After 2h of exposure, 3 shoots per treatment were snap-frozen in liquid nitrogen, ground and total RNA was extracted using TRI Reagent (Sigma-Aldrich, Buchs, Switzerland) following provider's instructions. RNA concentration was determined by Qubit (Life technologies, Zug, Switzerland) and quality was assessed by agarose gel electrophoresis and bioanalizer (Agilent, Santa Clara, Ca, USA). Total RNA extractions were done in triplicates.

RNA-Seq

Libraries of cDNA were prepared using the TruSeq mRNA stranded kit following manufacturer's instructions and sequenced on Illumina HiSeq 2000 (Illumina, San Diego, CA, USA) with 0.5-1 µg as total RNA input. *De novo* assembling of the transcriptome was realized with the 5 to 30 million 100 bp-length single reads obtained per sample using the module Oases (version 0.2.08; http://www.ebi.ac.uk/~zerbino/oases/) in Velvet (version 1.2.07;http://www.ebi.ac.uk/~zerbino/velvet/). We obtained 181'663 contigs on which samples reads were mapped and counted using MAQ (Mapping and Assembling with Qualities; version 0.7.1) with a success of 69 to 72 % mapping. Differential gene expression analyses were then done on the 99'030 contigs that had a minimum coverage of 20 reads in at least one sample. Counts were normalized by contig length and library size. Comparison of contig abundance, i.e. differential gene expression (DGE), was analyzed in CLC Main Workbench 7.7.1 (https://www.qiagenbioinformatics.com/) with the EdgeR Bioconductor package, generating fold change (FC) and false discovery rate corrected p-values (FDR). We defined significantly differently expressed contigs at a threshold of FDR <0.1% (Table S1).

Reads data were submitted to the NCBI public database (PRJEB6266), while raw data and project details can be found on the ArrayExpress archive (EMBL) under the accession E-MTAB-2557.

Targeted transcriptome analysis

A subset of contigs was selected based on *RNA-Seq* analysis and their expression level further analyzed by nCounter (nanoString, Seattle, WA, USA) using 1 µg total RNA. We designed a codeset with 29 genes, including 3 reference genes showing a constant expression in the different IHg and MeHg treatments (Table S2). The set also included 8 positive and 8 negative controls for background correction. 100 bp-long probes were designed with geneious v8

(www.geneious.com, Biomatters, Auckland, NZ) [12] and their specificity was tested against the whole transcriptome. Normalization of the signal was performed using geNorm [13]. FC were calculated comparing the geometric means (n=3 replicates) of exposed samples *vs Control*.

Annotation of biological functions

The *de novo* transcriptome was submitted to the Mercator plant database [14] and we performed a blast*x* search against the Viridiplantae (green plants) protein database of the National Center for Biotechnology Information (NCBI).

Effects of IHg and MeHg on chlorophyll, anthocyanin and anti-oxidative stress enzyme

Chlorophyll and anthocyanin contents were assessed by spectrophotometry as described in detail elsewhere [15]. Briefly, for chlorophyll, after extraction in 80 % acetone in the dark, absorbance of the extract was measured at 663 and 647 nm and µg of chlorophyll calculated using the formula: $(DO_{663nm} \times 7.15) + (DO_{647nm} \times 18.71)$. For anthocyanin, after extraction in 1 % methanol-HCl, absorbance of the extract was measured at 530 and 657 nm and µg of anthocyanin calculated using the formula: $DO_{530nm} - (DO_{657nm} \times 0.25)$.

The activities of class III peroxidases (POD) and superoxide dismutases (SOD) were measured as described in detail elsewhere [16]. Briefly, 20-50 mg of frozen ground plants were homogenized in 0.3 mL buffer containing 7.76 $g \cdot L^{-1}$ potassium phosphate, 584 $mg \cdot L^{-1}$ EDTA, 391 $mg \cdot L^{-1}$ mercaptoethanol and 0.5% Triton X-100. After centrifugation (10 min, 13'000*g*, 4° C), the supernatant was isolated and the activity of SOD and POD were measured by spectrophotometry.

Hg and Cu uptake

After exposure, shoots were washed with 1 mM EDTA if exposed to IHg or Cu, and 1 mM EDTA + 1 mM cysteine if exposed to MeHg, to assess intracellular (i.e. not extractable portion) metal concentrations [4]. Three shoots of plants were rinsed only with MilliQ water (*unwashed*), to calculate *adsorbed metal concentrations* by subtracting *washed* value to *unwashed* value.

For total Hg (THg = IHg + MeHg), lyophilized (Beta 1-8 K, Christ, Germany) shoots were analyzed by AMA-254 (Altec s.r.l., Czech Republic).

Plants exposed to MeHg for RNA-Seq were in addition analyzed for their MeHg concentration. MeHg concentrations were measured with a MERX-M Automated Methylmercury Analytical System (Brooks Rand Instruments, Seattle, WA, USA) following the US EPA Method 1630 [17] and manufacturer's instructions after mineralization 12h at 60 °C with 30 % HNO_3 (suprapur, Merck, Darmstadt, Germany).

Water samples were analyzed for their effective THg, MeHg and Cu concentrations (Table S3) with a MERX-T Automated Total Hg Analytical System (Brooks Rand Instruments, Seattle, WA, USA) [18], a MERX-M (see above) and an ICP-MS (7700x, Agilent Technologies, Morges, Switzerland), respectively.

Data analyses

Venn diagrams were built on http://bioinformatics.psb.ugent.be/webtools/Venn/. To compare the different treatments for whole transcriptome analysis and to find enriched pathways and transporters, we normalized the number of significantly contigs by the number of contigs that were assigned to a specific category in the whole *de novo* transcriptome. The biological

pathways of the significantly regulated contigs were visualized in MapMan (Version 3.6.0RC1; http://mapman.gabipd.org) [19, 20]. Contigs showing a dose-dependent response according to Hg uptake were selected manually in Excel (Microsoft, Redmond, WA, USA). Heatmaps and cluster analyses were performed in Genesis [21]. Statistics (t-tests), scatter, bar, radar and box plots were done in SigmaPlot 12.5 (Systat Software GmbH, Erkrath, Germany).

Results and Discussion

The aim of the first set of experiments was to compare uptake, whole transcriptome (RNA-Seq) and physiological responses in shoots exposed to 0.015, 0.15 and 15 $\mu g \cdot L^{-1}$ IHg and 0.01, 0.10, 1 or 10 $\mu g \cdot L^{-1}$ MeHg to determine and compare molecular toxicity pathways of IHg and MeHg.

Uptake of IHg and MeHg

Intracellular bioaccumulation of total Hg (THg= IHg + MeHg) and MeHg was measured at the end of the 2h-long exposure. A strong linear relationship (r^2=0.99) was evidenced between intracellular $[THg]_{intra}$ and $[THg]_{med}$ considering all IHg and MeHg treatments (Figure 1A, Tables S3 and S4). This supported that uptake of IHg and MeHg were similar in shoots. This observation differs from a study conducted in *E. nuttallii* exposed to IHg and MeHg in natural water showing a 10× higher accumulation of MeHg than IHg at similar exposure concentrations [7], as well as from results of field studies generally showing a 2-4× higher bioaccumulation of MeHg than IHg [3]. On the other hand these results are in line with data concerning *E. nuttallii* that showed a particularly high IHg bioaccumulation in this species in the field [7], and with the observation of comparable intracellular contents in the green microalga *Chlamydomonas reinhardtii* exposed 48h to mixtures in the $pg \cdot L^{-1}$ to $ng \cdot L^{-1}$ range of ^{199}IHg and ^{201}MeHg in an artificial medium without DOM [22]. These observations suggest that binding to DOM is a central factor for IHg and MeHg uptake in biota in natural waters.

Moreover, here ratios of *unwashed*:*washed* shoots were higher for IHg (3, 1.2 and 1.4 for 0.015, 0.15 and 15 $\mu g \cdot L^{-1}$ IHg, respectively) than for MeHg (1 for the 4 concentrations) (Table S4). This observation supports a stronger affinity of IHg to extracellular binding sites of cell walls. Indeed, cell walls are known to play a central role in plant tolerance to toxic metals: for example 80 % of Hg was accumulated in the cell walls in willow [23]. In the same line, a previous study in *E. nuttallii* measured an increased proportion over time of IHg in cell walls, concomitantly with an increased lignification of cell walls after 7 d exposure to 200 $ng \cdot L^{-1}$ IHg [4]. Data globally suggest that in *E. nuttallii*, cell wall binding is higher for IHg than MeHg, while uptake of IHg and MeHg are similar in the absence of DOM. In natural waters with low Hg concentrations, it is thus likely that the binding of IHg to DOM and cell walls reduces IHg uptake compared to MeHg.

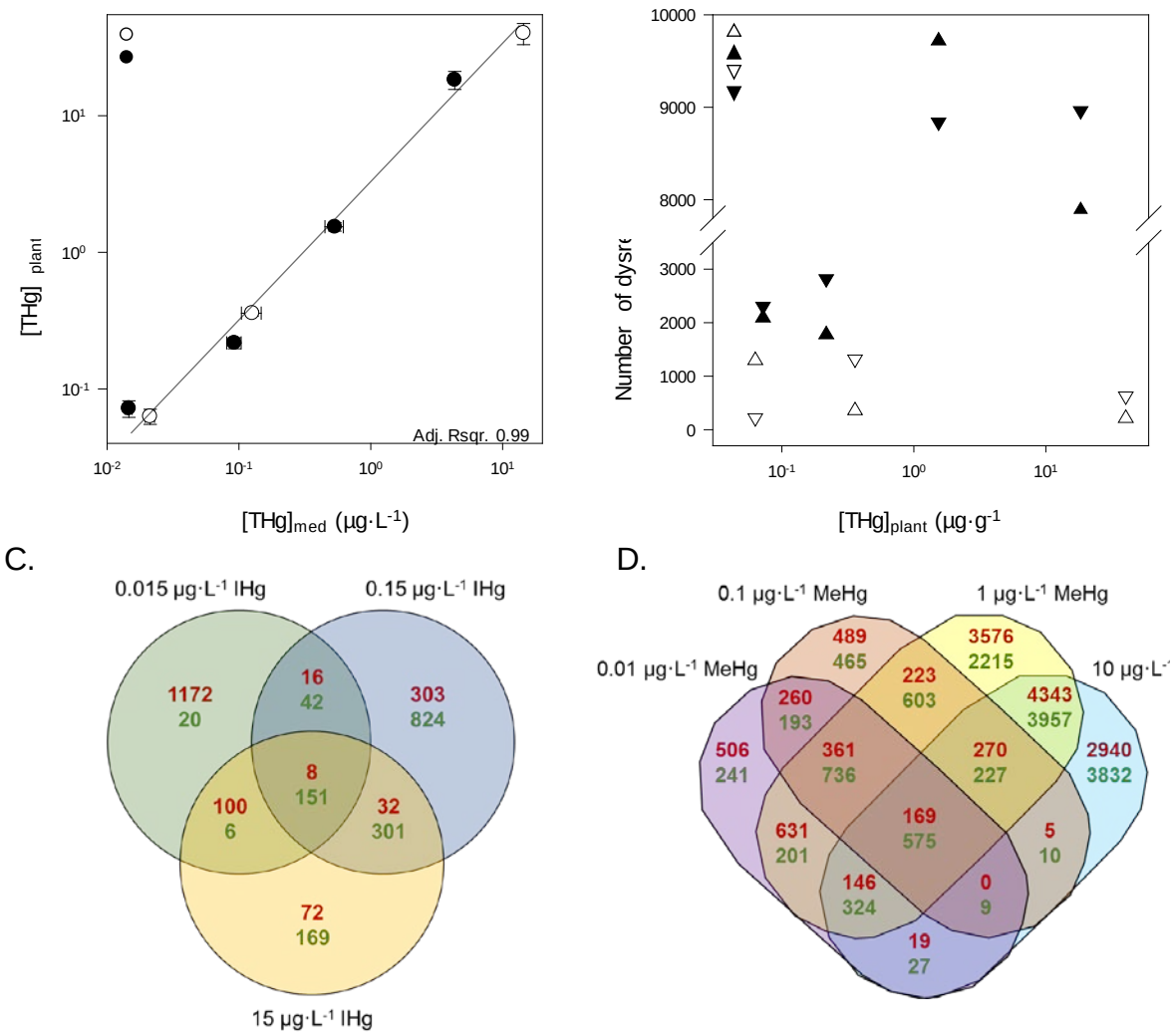

Figure 1. Uptake of IHg (white) and MeHg (black) in washed *E. nuttallii* measured as total Hg (THg = IHg + MeHg) *vs* effective concentration of IHg and MeHg in media (n=3) (A); Number of contigs significantly up- or down-regulated (FDR < 0.1 %) *vs* bioaccumulated THg (dw, dry weight) (B). Venn diagrams of the significantly differentially regulated contigs in *Elodea nuttallii* exposed 2 h to (C) IHg or (D) MeHg. (upregulated, red and upper numbers; downregulated, green and lower numbers; FDR < 0.1 %).

Differential gene expression analysis by RNA-Seq

The number of reads ranged between 6.3 and 23.9 million, with 69.1 to 73.0 % mapping (Table S4). Exposure to IHg resulted in a relatively stable impact on the transcriptome along the 3 orders of concentrations, with the regulation of up to 1'677 contigs for 0.36 $\mu g_{THg} \cdot g^{-1}$ dry weight (dw; Figure 1B, Table S4). This is comparable with a previous study in *E. nuttallii* exposed to 0.077 and 77 $\mu g \cdot L^{-1}$ IHg (intracellular concentrations of 0.1 and 170 $\mu g_{THg} \cdot g^{-1}{}_{dw}$), resulting in a significant regulation of 127 and 6'745 contigs, respectively [16]. Increased THg uptake after MeHg exposure here resulted in the regulation of up to 18'557 contigs for 1.54 $\mu g_{THg} \cdot g^{-1}{}_{dw}$ and 16'853 for 18.3 $\mu g_{THg} \cdot g^{-1}{}_{dw}$ (Figure 1B, Table S4). For both IHg and MeHg, we observed a bell shape relationship between the number of significantly regulated contigs

and intracellular THg concentration (Figure 1C). Nevertheless, at close intracellular concentrations (e.g. 0.36 $\mu g_{THg} \cdot g^{-1}_{dw}$ for 0.15 $\mu g \cdot L^{-1}$ IHg and 0.22 $\mu g_{THg} \cdot g^{-1}_{dw}$ for 0.1 $\mu g \cdot L^{-1}$ MeHg), the number of contigs regulated by MeHg was 3× higher than by IHg (Figure 1B, Table S4). A similar observation was made previously for the microalga *Chlamydomonas reinhardtii*: 12× more regulated genes by MeHg than IHg at similar intracellular concentrations [24]. This supports that MeHg exposure results in higher gene regulation than IHg at similar intracellular concentration.

Functional annotation of the regulated contigs

Significantly regulated contigs were analyzed to identify and compare biological pathways impacted by the range of IHg and MeHg accumulation tested here (Table 1). For all treatments, unknown contigs represented the higher proportion (38 ± 10%) of regulated contigs, followed by contigs involved in gene regulation (DNA, RNA, protein, signaling; 26 ± 3 %), suggesting that despite the short-term exposure a significant modification of the transcriptome was occurring, supporting molecular effect of both Hg form. Other contigs were attributed to cell structure (cell processes, cell wall, development; 8 ± 1 %), energy metabolism (7 ± 3 %), transport (5 ± 2 %), stress (3 ± 1 %), secondary metabolism (2 ± 1 %), amino acid metabolism (2 ± 1 %) and redox (1 ± 0.2 %). Other categories represented less than 1 % of regulated contigs. Although the number of regulated contigs was very variable depending on the exposure concentrations and Hg form, all treatments tested here gave very similar proportions of regulated contigs in the main GO categories. This suggests that increasing intracellular concentrations amplified the impact, but did not seemed to result in new cellular targets. Moreover, among all the treatments, 3’216 and 27’288 contigs were regulated by IHg and MeHg respectively. 2’983 contigs were common to both Hg forms, representing 93 % of the IHg- and 11 % of the MeHg-regulated contigs, resulting in 233 and 24’305 specific regulated contigs by IHg and MeHg, respectively. Half of the contigs specifically regulated by IHg had unknown functions and 30 % were involved in gene expression and cell processes. Other contigs were assigned to transport (10 %), energy metabolism (photosynthesis, sugars and ATP synthesis, 5 %) amino acid metabolism (3 %), redox (2 %), secondary metabolism (2 %), hormone and lipid metabolisms (1 % each) and cell wall (0.5 %). Contigs specifically regulated by MeHg were assigned to unknown functions (41 %), gene expression and cell processes (35 %), transport (4 %), energy metabolism (5 %), hormone and lipid metabolisms (2 % each), amino acid metabolism (1 %), redox (1 %), secondary metabolism (1 %), and cell wall (2 %). In sum, although different contigs were regulated by MeHg compared to IHg, they were found in the same categories of GO.

Main biological pathways regulated by IHg and MeHg

To estimate the importance of those regulations, we in addition calculated the proportion of regulated contigs *vs* identified contigs in the *de novo* transcriptome for each category. Contigs involved in polyamine metabolism, sugars metabolisms (i.e. gluconeogenesis, glycolysis), secondary metabolism and cell wall concerned a significant proportion of contigs identified in those categories in *E. nuttallii* (Figure 2, Table S5). For example, 10 $\mu g \cdot L^{-1}$ MeHg resulted in the regulation of 51.7 % of contigs involved in polyamine metabolism. Polyamines (PAs) are low-molecular weight aliphatic polycations (e.g. putrescine, spermidine). In the same line, increased polyamine content and decreased activity of the polyamine oxidase was reported in

leaves of the water hyacinth after 6 days of exposure to 6 mg·L^{-1} IHg [25]. PAs have a protecting effect on membranes against oxidative stress [26, 27]. PAs might therefore be involved in the tolerance response of *E. nuttallii* to IHg and MeHg.

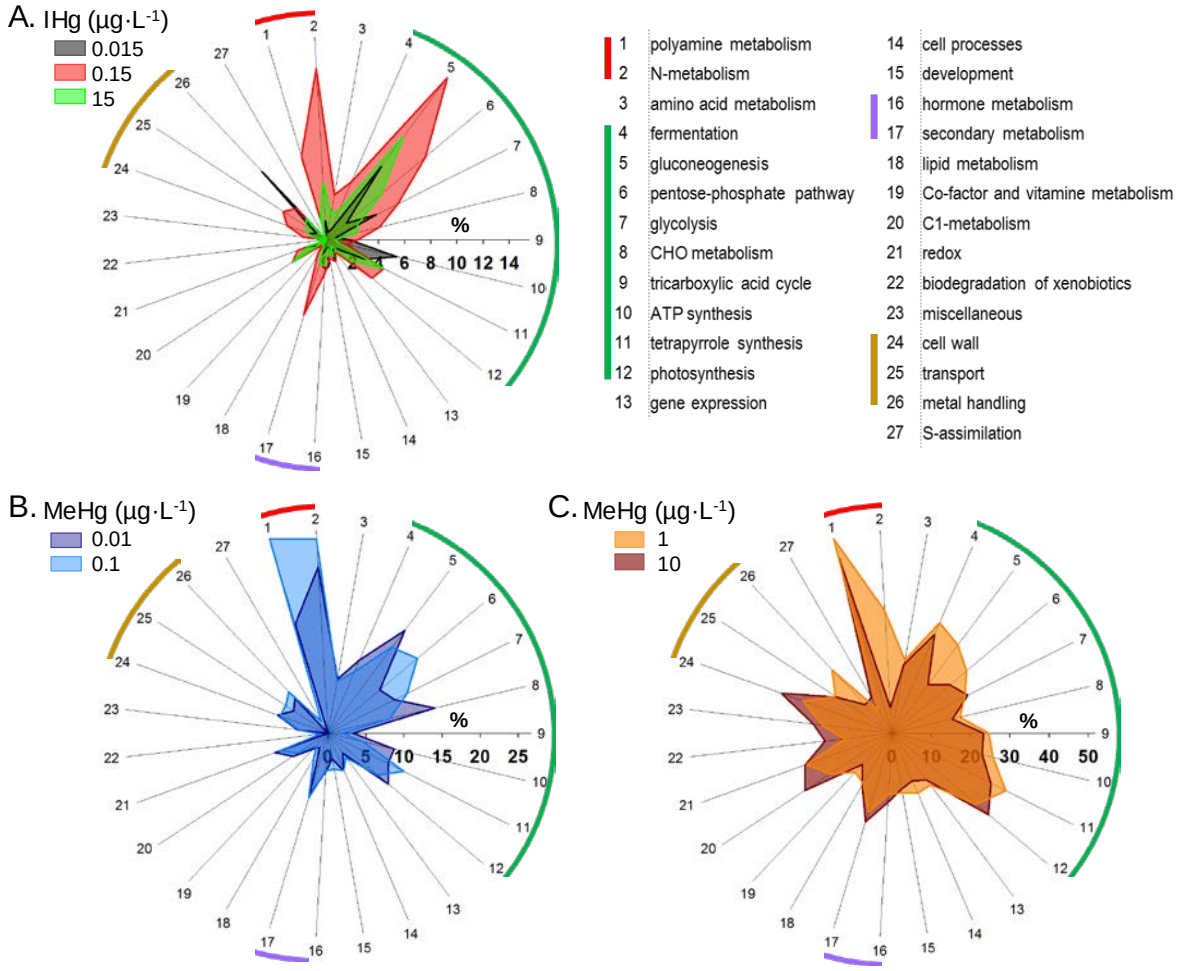

Figure 2. Biological pathways (MapMan) of the significantly regulated contigs (FDR < 0.1 %) by 0.015, 0.15 and 15 µg·L^{-1} IHg (A), 0.01 and 0.1 µg·L^{-1} MeHg (B) or 1 and 10 µg·L^{-1} MeHg (C) shown as a proportion (%) of the number of contigs attributed to the category in the whole *de novo* transcriptome. Raw counts are given in Table S5.

Contigs involved in *energy metabolism* were highly regulated by both IHg and MeHg (Table 1, Figure 2). Namely, we observed the up-regulation of 15, 74 and 107 contigs involved in glycolysis at 0.15 µg·L^{-1} IHg, 1 and 10 µg·L^{-1} MeHg, respectively. The number of regulated contigs involved in gluconeogenesis was relatively stable between the different IHg and MeHg treatments (5, 11, 7 at 0.015, 0.15 and 15 µg·L^{-1} IHg, 12, 10, 20 and 11 at 0.01, 0.1, 1 and 10 µg·L^{-1} MeHg) (Figure 2). Globally, contigs involved in sugar metabolisms (minor and major carbohydrate metabolisms, gluconeogenesis, fermentation) were down-regulated in response to IHg, except glycolysis and tricarboxylic acid cycle at 0.15 µg·L^{-1} IHg. Similarly, 0.01 and 0.1 µg·L^{-1} MeHg treatments down-regulated most contigs involved in sugar metabolisms, while 1 and 10 µg·L^{-1} MeHg up-regulated most contigs involved in sugar metabolisms (e.g. pentose-phosphate pathway, 18, 29, 21 and 6 contigs down-regulated, 0, 2, 29 and 33 contigs up-regulated at 0.01, 0.1, 1 and 10 µg·L^{-1} MeHg). In the same line, contigs involved in the

biogenesis of the photosystem II (PSII) were up-regulated at 1 and 10 µg·L^{-1} MeHg (e.g. Locus_1310_Transcript_4_9, PSII stability/assembly factor), while this function was not present in the contigs significantly regulated by the other treatments (Table S5). We observed an up-regulation of contigs involved in photorespiration only at 10 µg·L^{-1} MeHg: 56 up-, 13 down-regulated contigs *vs* 4 up- and 26 down-regulated contigs at 0.1 µg·L^{-1} MeHg for example (Table S5). Furthermore, the expression of contigs involved in chlorophyll b synthesis was regulated by MeHg exposure (e.g. Locus_3359, log2FC 0.9, 0.8, 1.4 and 0.8 at 0.01, 0.1, 1 and 10 µg·L^{-1}MeHg and Locus_70977_transcript_2_2, log2FC -4.0 and 1.1 at 0.01 and 10 µg·L^{-1} MeHg) but was not significantly regulated in IHg treatments. The strong response of contigs involved in energy metabolisms observed here was consistent with the expected impact of Hg at higher concentrations and consistent with previous studies both at the transcriptomic and proteomic levels in *E. nuttallii* [4, 10, 24].

As mentioned earlier, *Cell structure* is affected by Hg and *Cell wall* is important for Hg tolerance. At the gene-level, the leucine-rich repeat proteins -involved in the structure of the cell wall [28]- were all down-regulated (2 contigs at 0.015 and 15 µg·L^{-1} IHg, 4 at 0.15 µg·L^{-1} IHg and 16 to 48 from 0.01 to 10 µg·L^{-1} MeHg). Cell wall precursors synthesis were also impacted by IHg and MeHg, and the response was higher for MeHg than IHg, and increased from 0.01 to 10 µg·L^{-1} MeHg (up to 3 contigs for 0.15 µg·L^{-1} IHg, 10, 12, 60 and 59 contigs for 0.01 to 10 µg·L^{-1} MeHg, respectively). The cellulose synthase pathway, was down regulated in all treatments, except at 10 µg·L^{-1} MeHg, where 23 contigs were up-regulated, showing here a specificity of the response to high MeHg treatment. Contigs coding for pectin esterases and pectin methyltransferases were also strongly regulated by MeHg treatments (Table S5). These results are in line with previous studies showing a modification of cell wall composition and structure by the exposure to IHg and MeHg [4].

The expression of *transporters* can give insight on internalization and detoxification mechanisms. Contigs coding for vacuolar ATPases were both up- and down-regulated at every MeHg concentration, while mostly down-regulated by IHg (Table 2). At 10 µg·L^{-1} MeHg, half on the contigs assigned to vacuolar proton (H^+) transporting pyrophosphatases in the *de novo* transcriptome were up-regulated (e.g. Locus_606_Transcript_13_14, pyrophosphate-energized vacuolar membrane proton pump-like, log2FC 0.7 and 1.0 at 1 and 10 µg·L^{-1} MeHg). Data point thus to an increased vacuolar transport with increasing Hg accumulation in shoots, suggesting that compartmentation in vacuoles could be a tolerance mechanism in *E. nuttallii*. Indeed the vacuoles are known to be the final destination for metals in plants both as free ions or bound with specific molecules such as phytochelatins (PCs) [29]. In the same line, in response to IHg, a high proportion of contigs coding for ABC and metabolites transporters were regulated. Contigs coding for S transporters were down-regulated at 0.1, 1 and 10 µg·L^{-1} MeHg and at 0.15 µg·L^{-1} IHg, while up-regulated at 10 µg·L^{-1} MeHg. In response to MeHg, numerous contigs coding for porins, proteins, nutrients (calcium, potassium), anions (e.g. Cl^-, HCO_3^-) and cations (e.g. Mg^{2+}, Na^+) were regulated (Table 1). Contigs coding for nitrate and ammonium transporters were down-regulated by IHg and MeHg, except at 10 µg·L^{-1} MeHg. Data suggest thus that Hg treatments might globally impact nutrition in *E. nuttallii*. In the same line, a study showed in *C. reinhardtii*, exposed 4-d to 33.6 mg·L^{-1} cadmium a reduction of algal N content by 20 % [30].

Secondary metabolism was a category showing a high proportion of regulated contigs by IHg and MeHg (Table 1, Figure 2). Contigs involved in lignin biosynthesis were down-regulated with 28, 25, 29 and 31 assigned contigs for MeHg and 5, 22 and 7 for IHg (e.g. phenylalanine ammonia-lyase 1, Locus_346_transcript_11_12, log_2FC -1.9 at 0.01 µg·L^{-1} MeHg, -1.0 at 0.015 µg·L^{-1} IHg, -1.6 at 0.1 µg·L^{-1} MeHg, -1.4 at 0.15 µg·L^{-1} IHg, -2.6 at 1 µg·L^{-1} MeHg, -0.9 at 10 µg·L^{-1} MeHg and -1.4 at 15 µg·L^{-1} IHg; 4-coumarate-CoA ligase 2, Locus_39536_transcript_1_5, log_2FC -1.2 at 0.015 µg·L^{-1} IHg, -1.2 at 0.15 µg·L^{-1} IHg, -1.6 at 15 µg·L^{-1} IHg, -2.3 at 0.01 µg·L^{-1} MeHg, -1.4 at 0.1 µg·L^{-1} MeHg, -2.0 at 1 µg·L^{-1} MeHg). Contigs involved in the anthocyanin pathway were also regulated by MeHg (6 down, 1 up and 9 down, 1 up for 1 and 10 µg·L^{-1} MeHg, respectively). Anthocyanins are phenolic secondary metabolites acting as antioxidants. Similarly, secondary metabolism was among the most enriched up-regulated pathway in a RNA-Seq study conducted in *E. nuttallii* exposed to 0.07, 80 and 800 µg·L^{-1} IHg [10], likely pointing to their important role in Hg tolerance.

Pigment content and anti-oxidative stress enzymes

To assess the impact of IHg and MeHg exposures at the cell level, several physiological endpoints were assessed (Table 3). A significant decrease in the chlorophyll content was measured after 2h exposure to 0.15 and 15 µg·L^{-1} IHg, while MeHg had non-significant effect on this endpoint (Table 3). This observation is congruent with transcriptome analysis, which showed a higher proportion of contigs involved in energy metabolism by those 2 IHg treatments than other treatments (Table 1).

Impaired photosynthesis and metal phytotoxicity are known to often trigger oxidative stress. We thus measured the activity of two key anti-oxidant enzymes, superoxide dismutases (SOD) and class III peroxidases (POD). A significant increase (1.7×) in SOD activity was observed in shoots exposed 2h to 0.15 µg·L^{-1} IHg, while it was non-significant for other treatments. In shoots exposed to 0.1 and 1 µg·L^{-1} MeHg, we observed a 3.3× and 2.4× increase of POD activity, respectively. Finally, the content of the pigment anthocyanin, a non-enzymatic anti-oxidant compound (secondary metabolite), was determined because of its role in tolerance to reactive oxygen species (ROS) [31]. An increase of 4.8× to 7.6× at 0.01 and 10 µg·L^{-1} MeHg *vs* control of anthocyanin content was observed, while no significant effect on this pigment was measured for IHg when exposed 24h to 0.077 and 77 µg·L^{-1} IHg *vs* control (80.6 ± 23.7% and 59.0 ± 7.9%, for 0.077 and 77 µg·L^{-1} IHg, respectively) [16]. This suggests that increase of anthocyanin content was specific to MeHg exposure. In RNA-Seq analysis, contigs involved in the anthocyanin biosynthesis pathway were mostly down-regulated, which may be a retroactive regulation [32]. Similarly in *Arabidopsis thaliana* seedlings, exposure to 60 mg·L^{-1} IHg induced a 10× increase in anthocyanin content [33]. Arsenic stress increased anthocyanin content in *Lemna gibba* [31].

To summarize, data in *E. nuttallii* suggested that both enzymatic and non-enzymatic anti-oxidant defenses were triggered by MeHg treatments, certainly to cope with an increase of ROS, while IHg treatments resulted in a higher binding in cell walls and decreased chlorophyll content.

Mixture exposures and targeted transcriptome analysis

We further selected in RNA-Seq analysis a subset of contigs showing an expression level congruent with Hg uptake. The aim was to improve environmental realism by characterizing Hg uptake and targeted transcriptomic in mixtures, i.e. in the presence of SRHA and Cu. 100

contigs were selected because of their functions in the main impacted biological pathways and because they responded in a dose-dependent manner with increasing IHg or MeHg exposure. After quality control and removal of contigs showing a log_2FC >0.5 in *1 mg·L^{-1} SRHA* and *10 mg·L^{-1} SRHA*, 16 contigs passed quality control (Table S2). This subset included contigs coding for a catalase, the PSI subunit, two pectinesterases, 4-coumarate-ligase and 2 S-adenosylmethionine (SAM) enzymes, involved in the biosynthesis of secondary metabolites.

Uptake of Hg in mixture with MeHg, Cu and SRHA

In the absence of SRHA, mixture with Cu at both 0.15 and 15 µg·L^{-1} IHg decreased IHg uptake. More in detail, the ratio $[THg]_{plant}/[THg]_{med}$ decreased 5.5× and 4× for 0.15 and 15 µg·L^{-1} IHg, respectively (Figure 3A). THg uptake at 0.25 µg·L^{-1} MeHg in presence of Cu was halved (Figure 3B). These observation confirmed a previously suspected competition between Cu and Hg in *E. nuttallii* [7].

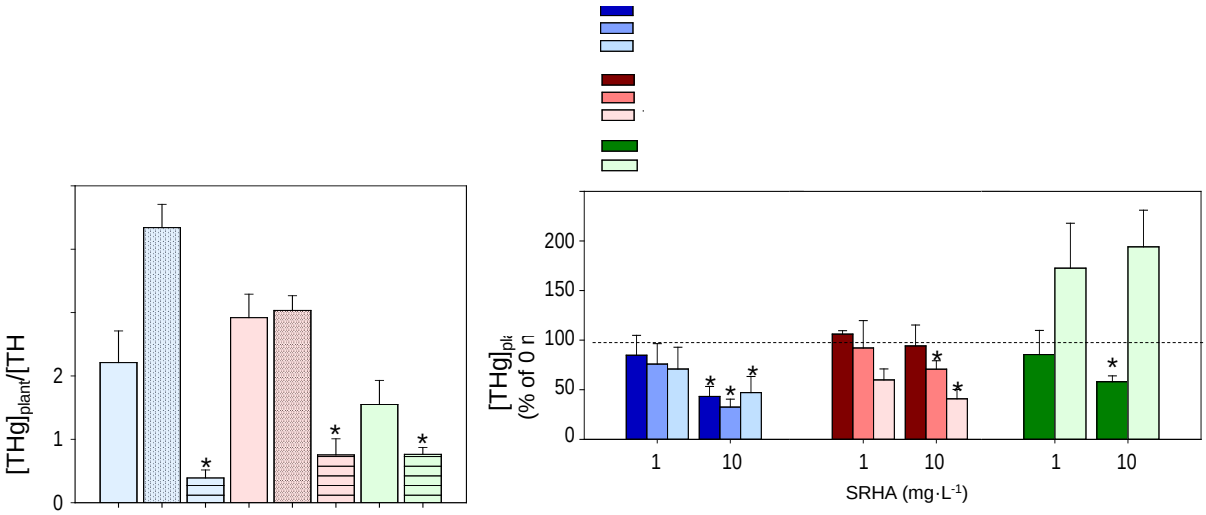

Figure 3. Effect of Cu or MeHg on IHg uptake and of Cu on MeHg uptake in absence (A) and presence of SRHA (B). Uptake was measured as THg (= IHg + MeHg) concentration in washed plants ($[THg]_{plant}$) and divided by THg concentration in medium ($[THg]_{med}$) at the beginning of the exposure. Asterisks indicate a significant difference with the respective treatment without competitor (A) or with the respective treatment without SRHA normalized to 100% (dashed line) (mean ± SD, n = 3, t-test, *p*-value <0.05).

The addition of 1 mg·L^{-1} SRHA had non-significant impact on THg uptake in all treatments. The addition of 10 mg·L^{-1} SRHA in both 0.15 µg·L^{-1} IHg and 0.25 µg·L^{-1} MeHg treatments decreased significantly THg uptake, while it had non-significant effect on THg uptake at 15 µg·L^{-1} IHg (Figure 4). For both mixtures IHg + MeHg and IHg + Cu, 10 mg·L^{-1} SRHA reduced significantly THg uptake (32 and 71 % of THg uptake in absence of SRHA in 0.15 µg·L^{-1} IHg + 0.25 µg·L^{-1} MeHg and 15 µg·L^{-1} IHg + 0.25 µg·L^{-1} MeHg, respectively), whereas for MeHg + Cu mixture, we measured a significant 1.9× increase in THg uptake.

The presence of dissolved organic matter (DOM), had both been reported to increase or decrease Hg bioaccumulation, depending on DOM characteristics and concentration [34-36].

Presence of sulphur containing ligands and humic acid (HA) increased Hg uptake in *Brassica juncae* [37]. In lettuce, HA reduces Hg uptake by the formation of complexes and consequently reduced the inhibition of chlorophyll by Hg [38], but HA decreased Cu toxicity in lettuce sprouts without decreasing Cu uptake [39]. DOM was significantly less effective at reducing Hg toxicity than Cu toxicity in a marine bacterium (*Vibrio fischeri*), most certainly because Hg and Cu interact differently with DOM. Indeed at environmentally relevant concentrations, Cu is preferentially bound to nitrogen and oxygen ligands, while Hg binds first to thiol groups and reduced sulfur [35, 40]. When the high-affinity S binding sites become saturated, Hg binds to oxygen functional groups with lower affinity [36, 41-43]. Here difference between Cu + IHg and Cu + MeHg may rely on different affinities of Hg species to DOM.

The speciation modeling predicted 99-100 % of IHg to be bound to SRHA, thus an extremely low abundance of the free Hg ion was estimated (Table S6). While no effect of 1 $mg \cdot L^{-1}$ SRHA on THg uptake was observed for 15 $\mu g \cdot L^{-1}$ IHg and 15 $\mu g \cdot L^{-1}$ IHg + 0.25 $\mu g \cdot L^{-1}$ MeHg, for which [S]/[Hg] was 0.03, we observed a significant impact of 10 $mg \cdot L^{-1}$ SRHA on THg uptake for 0.25 $\mu g \cdot L^{-1}$ MeHg, resulting in a [S]/[Hg] ratio of 1150. Data are thus in line with the expected decrease of Hg uptake by binding to S groups in SRHA. For MeHg + Cu mixture and more generally in the literature, effect of HA on Hg uptake is rather complex making generalizations difficult. Indeed, although interactions of Hg with biological ligands are known to determine Hg bioavailability, they are dependent of multiple factors (e.g. ligands, pH) making modeling of Hg bioavailability currently a challenge [44].

Effect of SRHA on the gene signature of effect-oriented biomarkers

The expression level of the selected contigs was analyzed in the absence and presence of SRHA (Figure 4). All contigs were regulated in presence of SRHA and in mixtures. Hierarchical clustering of all contigs expression level were analyzed for its potential as ecotoxicogenomic tool to assess exposure in mixtures. In the absence of SRHA, the hierarchical clustering of contigs signature resulted in a good discrimination of the samples exposed to Cu from the other treatments, and of IHg from MeHg (Figure 4). In response to IHg exposure, 9 genes were up-regulated (e.g. Locus_8381, 4-coumarate ligase and DNA polymerase) at 0.15 and 15 $\mu g \cdot L^{-1}$ IHg, and 4 were up-regulated only at higher IHg concentration, namely the catalase, SAM carrier 1 and pectinesterases. This result was in line with the RNA-Seq results (e.g. cell wall metabolism). The IHg-MeHg mixtures, however, were clustered closer to MeHg than IHg treatments, suggesting a higher sensitivity of the selected contigs to MeHg than IHg. On the opposite, MeHg + Cu was clustered next to Cu, certainly because of the down-regulation of Locus_8381 and the receptor kinase which showed specificity to Cu exposure.

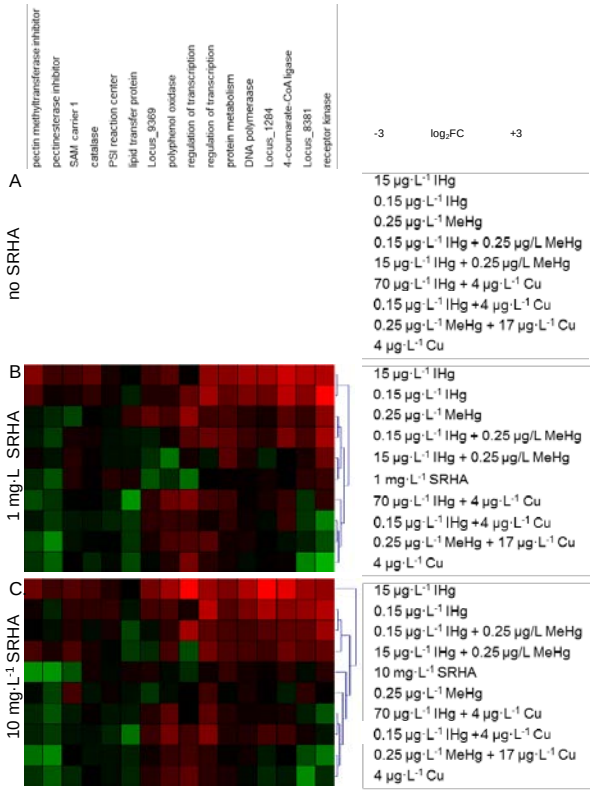

Figure 4. Hierarchical clustering (average linkage, Euclidean distance) of differential expression level of selected contigs in the different mixture scenarios in the absence (A) or presence of 1 mg·L^{-1} (B) or 10 mg·L^{-1} SRHA (C) (SAM, S-adenosyl-methionine; PSI, photosystem I).

The addition of 1 mg·L^{-1} SRHA didn't influence the clustering of the samples (Figure 4), in line with its non-significant effect on the uptake. The signature of 1 mg·L^{-1} SRHA alone was close to 15 µg·L^{-1} IHg + 0.25 µg·L^{-1} MeHg. In the presence of 10 mg·L^{-1} SRHA, the signature of 15 µg·L^{-1} IHg treatments was significantly distinct from the other treatments (Figure 4) that formed 2 big clusters. The signature of 10 mg·L^{-1} SRHA alone was close to 0.25 µg·L^{-1} MeHg and Cu treatments. At this SRHA concentration, IHg and IHg + MeHg samples clustered together, suggesting that the MeHg-sensitivity was mitigated compared with signatures observed in the absence of DOM.

Cu uptake and altered gene expression in mixtures with Hg, MeHg and SRHA

In the absence of SRHA, the mixtures of Cu with IHg and MeHg significantly decreased intracellular Cu concentration. Cu uptake significantly increased when 1 mg·L^{-1} SRHA was added in mixtures, but not in Cu treatment only (t-test, *p*-value = 0.06; Figure S2). In presence of 10 mg·L^{-1} SRHA, the measured intracellular Cu concentration was not significantly different from the one in absence of SRHA, except for 17 µg·L^{-1} Cu + 0.25 µg·L^{-1} MeHg, for which Cu uptake significantly decreased (1.4×). These results confirmed the interaction between Cu and IHg/MeHg, in line with previously observed competition of Cu on THg uptake and increased THg, in MeHg + Cu mixtures.

In the absence of SRHA, Cu samples clustered according to measured Cu uptake, ranging from 2.20 ± 0.02 µg·g$^{-1}_{dw}$ in 70 µg·L^{-1} IHg + 4 µg·L^{-1} Cu to 6.37 ± 0.13 µg·g$^{-1}_{dw}$ in 4 µg·L^{-1} Cu (Figure 4). In the presence of 1 mg·L^{-1} SRHA, Cu uptake increased (*vs* in the absence of

SRHA), but the gene signature of 70 µg·L^{-1} IHg + 4 µg·L^{-1} Cu was closer to Hg samples and 1 mg·L^{-1} SRHA (Figure 4). Similarly, at 10 mg·L^{-1} SRHA, although Cu uptake decreased in 17 µg·L^{-1} Cu + 0.25 µg·L^{-1} MeHg *vs* 17 µg·L^{-1} Cu, non-significant change in the gene expression signature was observed and Cu treatments were identically clustered than for other SRHA concentrations, (Figures 4 and S1).

Data thus suggested that the subset of selected genes responded more specifically to Hg than to Cu. However, gene signature successfully discriminated IHg, MeHg and Cu treatments in mixtures in presence of DOM. Our data confirmed the hypothesis that transcriptomic is a very sensitive approach, and is promising for deriving biomarkers of exposure in environmentally relevant scenarios, for example, in mixtures at sublethal concentrations and should be further explored for its suitability for ecotoxicological testing.

Acknowledgments

The authors acknowledge the Swiss National Science Foundation for financial support (contracts 205321_138254 and 200020_157173), Drs. Mylène Docquier and Didier Chollet for nCounter analyses.

References

1. Boudou, A.; Maury-Brachet, R.; Coquery, M.; Durrieu, G.; Cossa, D., Synergic effect of gold mining and damming on mercury contamination in fish. Environ Sci Technol 2005, 39, (8), 2448-2454.

2. UNEP, Global Mercury Assessment 2013: Sources, Emissions, Releases and Environmental Transport. Geneva, Switzerland.

3. Bravo, A. G.; Cosio, C.; Amouroux, D.; Zopfi, J.; Chevalley, P.-A.; Spangenberg, J. E.; Ungureanu, V.-G.; Dominik, J., Extremely elevated methyl mercury levels in water, sediment and organisms in a Romanian reservoir affected by release of mercury from a chlor-alkali plant. Water Res 2014, 49, 391-405

4. Larras, F.; Regier, N.; Planchon, S.; Pote, J.; Renaut, J.; Cosio, C., Physiological and proteomic changes suggest an important role of cell walls in the high tolerance to metals of *Elodea nuttallii*. J Hazard Mater 2013, 263, 575-83.

5. Beauvais-Fluck, R.; Chaumot, A.; Gimbert, F.; Queau, H.; Geffard, O.; Slaveykova, V. I.; Cosio, C., Role of cellular compartmentalization in the trophic transfer of mercury species in a freshwater plant-crustacean food chain. J Hazard Mater 2016, 320, 401-407.

6. Beauvais-Fluck, R.; Gimbert, F.; Mehault, O.; Cosio, C., Trophic fate of inorganic and methyl-mercury in a macrophyte-chironomid food chain. J Hazard Mater 2017, 338, 140-147.

7. Regier, N.; Larras, F.; Bravo, A. G.; Ungureanu, V. G.; Amouroux, D.; Cosio, C., Mercury bioaccumulation in the aquatic plant *Elodea nuttallii* in the field and in microcosm: accumulation in shoots from the water might involve copper transporters. Chemosphere 2013, 90, (2), 595-602.

8. Regier, N.; Frey, B.; Converse, B.; Roden, E.; Grosse-Honebrick, A.; Bravo, A. G.; Cosio, C., *Elodea nuttallii* roots effect on bacterial communities and MMHg proportion in a Hg polluted sediment. Plos one 2012, 7, (9), e45565.

9. Chen, Y. A.; Chi, W. C.; Trinh, N. N.; Huang, L. Y.; Chen, Y. C.; Cheng, K. T.; Huang, T. L.; Lin, C. Y.; Huang, H. J., Transcriptome profiling and physiological studies reveal a major role for aromatic amino acids in mercury stress tolerance in rice seedlings. Plos One 2014, 9, (5), e95163.

10. Regier, N.; Baerlocher, L.; Munsterkotter, M.; Farinelli, L.; Cosio, C., Analysis of the *Elodea nuttallii* transcriptome in response to mercury and cadmium pollution: development of sensitive tools for rapid ecotoxicological testing. Environ Sci Technol 2013, 47, (15), 8825-34.

11. Beauvais-Flück, R.; Slaveykova, V. I.; Cosio, C., Effects of two-hour exposure to environmental and high concentrations of methylmercury on transcriptome and physiology of the macrophyte *Elodea nuttallii*. Aquatic Toxicol 2017, *194*, 103-111.

12. Kearse, M.; Moir, R.; Wilson, A.; Stones-Havas, S.; Cheung, M.; Sturrock, S.; Buxton, S.; Cooper, A.; Markowitz, S.; Duran, C.; Thierer, T.; Ashton, B.; Meintjes, P.; Drummond, A., Geneious Basic: an integrated and extendable desktop software platform for the organization and analysis of sequence data. Bioinformatics 2012, 28, (12), 1647-9.

13. Vandesompele, J.; De Preter, K.; Pattyn, F.; Poppe, B.; Van Roy, N.; De Paepe, A.; Speleman, F., Accurate normalization of real-time quantitative RT-PCR data by geometric averaging of multiple internal control genes. Genome Biol 2002, 3, (7), Research0034.

14. Lohse, M.; Nagel, A.; Herter, T.; May, P.; Schroda, M.; Zrenner, R.; Tohge, T.; Fernie, A. R.; Stitt, M.; Usadel, B., Mercator: a fast and simple web server for genome scale functional annotation of plant sequence data. Plant Cell Environ 2014, 37, (5), 1250-8.

15. Cosio, C.; Dunand, C., Transcriptome analysis of various flower and silique development stages indicates a set of class III peroxidase genes potentially involved in pod shattering in *Arabidopsis thaliana*. Bmc Genomics 2010, 11, 16.

16. Regier, N.; Beauvais-Flück, R.; Slaveykova, V. I.; Cosio, C., *Elodea nuttallii* exposure to mercury exposure under enhanced ultraviolet radiation: Effects on bioaccumulation, transcriptome, pigment content and oxidative stress. Aquatic Toxicol 2016, 180, 218-226.

17. USEPA, Aquatic life ambient freshwater quality criteria- copper. US Environmental Protection Agency, 2007.

18. USEPA, Method 1631: Mercury in Water by Oxidation, Purge and Trap, and CVAFS. US Environmental Protection Agency, 2002.

19. Thimm, O.; Blasing, O.; Gibon, Y.; Nagel, A.; Meyer, S.; Kruger, P.; Selbig, J.; Muller, L. A.; Rhee, S. Y.; Stitt, M., MAPMAN: a user-driven tool to display genomics data sets onto diagrams of metabolic pathways and other biological processes. Plant J 2004, 37, (6), 914-39.

20. Usadel, B.; Poree, F.; Nagel, A.; Lohse, M.; Czedik-Eysenberg, A.; Stitt, M., A guide to using MapMan to visualize and compare Omics data in plants: a case study in the crop species, Maize. Plant Cell Environ 2009, 32, (9), 1211-1229.

21. Sturn, A.; Quackenbush, J.; Trajanoski, Z., Genesis: cluster analysis of microarray data. Bioinformatics 2002, 18, 207-208.

22. Bravo, A. G.; Le Faucheur, S.; Monperrus, M.; Amouroux, D.; Slaveykova, V. I., Species-specific isotope tracers to study the accumulation and biotransformation of mixtures of inorganic and methyl mercury by the microalga *Chlamydomonas reinhardtii*. Environ Poll 2014, 192, (0), 212-215.

23. Wang, Y.; Greger, M., Clonal differences in mercury tolerance, accumulation, and distribution in willow. J Environ Qual 2004, 33, (5), 1779-85.

24. Beauvais-Fluck, R.; Slaveykova, V. I.; Cosio, C., Cellular toxicity pathways of inorganic and methyl mercury in the green microalga *Chlamydomonas reinhardtii*. Scientific Reports 2017, *7*, 8034

25. Ding, C. X.; Shi, G. X.; Xu, X. Y.; Yang, H. Y.; Xu, Y., Effect of exogenous spermidine on polyamine metabolism in water hyacinth leaves under mercury stress. Plant Growth Regul 2010, 60, (1), 61-67.

26. Sharma, S. S.; Dietz, K.-J., The significance of amino acids and amino acid-derived molecules in plant responses and adaptation to heavy metal stress. J Exp Bot 2006, 57, (4), 711-726.

27. Groppa, M. D.; Tomaro, M. L.; Benavides, M. P., Polyamines and heavy metal stress: the antioxidant behavior of spermine in cadmium- and copper-treated wheat leaves. Biometals 2007, 20, (2), 185-95.

28. Draeger, C.; Fabrice, T. N.; Gineau, E.; Mouille, G.; Kuhn, B. M.; Moller, I.; Abdou, M. T.; Frey, B.; Pauly, M.; Bacic, A.; Ringli, C., *Arabidopsis* leucine-rich repeat extensin (LRX) proteins modify cell wall composition and influence plant growth. BMC plant biol 2015, 15.

29. Park, J.; Song, W. Y.; Ko, D.; Eom, Y.; Hansen, T. H.; Schiller, M.; Lee, T. G.; Martinoia, E.; Lee, Y., The phytochelatin transporters AtABCC1 and AtABCC2 mediate tolerance to cadmium and mercury. Plant J. 2012, 69, (2), 278-288.

30. Mosulen, S.; Dominguez, M. J.; Vigara, J.; Vilchez, C.; Guiraum, A.; Vega, J. M., Metal toxicity in *Chlamydomonas reinhardtii*. Effect on sulfate and nitrate assimilation. Biomolecular Engineering 2003, 20, (4-6), 199-203.

31. Leao, G. A.; de Oliveira, J. A.; Felipe, R. T. A.; Farnese, F. S.; Gusman, G. S., Anthocyanins, thiols, and antioxidant scavenging enzymes are involved in *Lemna gibba* tolerance to arsenic. J. Plant Interact. 2014, 9, (1), 143-151.

32. Dancs, G.; Kondrak, M.; Banfalvi, Z., The effects of enhanced methionine synthesis on amino acid and anthocyanin content of potato tubers. BMC plant biol 2008, 8.

33. Baek, S. A.; Han, T.; Ahn, S. K.; Kang, H.; Cho, M. R.; Lee, S. C.; Im, K. H., Effects of heavy metals on plant growths and pigment contents in *Arabidopsis thaliana*. Plant Pathol J 2012, 28, (4), 446-452.

34. Chiasson-Gould, S. A.; Blais, J. M.; Poulain, A. J., Dissolved organic matter kinetically controls mercury bioavailability to Bacteria. Environ Sci Technol 2014, 48, (6), 3153-3161.

35. Haitzer, M.; Aiken, G. R.; Ryan, J. N., Binding of mercury(II) to dissolved organic matter: the role of the mercury-to-DOM concentration ratio. Environ Sci Technol 2002, 36, (16), 3564-70.

36. Ravichandran, M., Interactions between mercury and dissolved organic matter - a review. Chemosphere 2004, 55, (3), 319-331.

37. Moreno, F. N.; Anderson, C. W.; Stewart, R. B.; Robinson, B. H.; Ghomshei, M.; Meech, J. A., Induced plant uptake and transport of mercury in the presence of sulphur-containing ligands and humic acid. New phytol 2005, 166, (2), 445-54.

38. Cozzolino, V.; De Martino, A.; Nebbioso, A.; Di Meo, V.; Salluzzo, A.; Piccolo, A., Plant tolerance to mercury in a contaminated soil is enhanced by the combined effects of humic matter addition and inoculation with arbuscular mycorrhizal fungi. Environ Sci Pollut Res Int 2016, 23, (11), 11312-22.

39. Inaba, S.; Takenaka, C., Effects of dissolved organic matter on toxicity and bioavailability of copper for lettuce sprouts. Environ Int 2005, 31, (4), 603-608.

40. Xia, K.; Bleam, W.; Helmke, P. A., Studies of the nature of Cu^{2+} and Pb^{2+} binding sites in soil humic substances using X-ray adsorption spectroscopy. Geochim Cosmochim Acta 1997, 61, (11), 2211-2221.

41. Hesterberg, D.; Chou, J. W.; Hutchison, K. J.; Sayers, D. E., Bonding of Hg(II) to reduced organic sulfur in humic acid as affected by S/Hg ratio. Environ Sci Technol 2001, 35, (13), 2741-5.

42. Skyllberg, U.; Bloom, P. R.; Qian, J.; Lin, C. M.; Bleam, W. F., Complexation of mercury(II) in soil organic matter: EXAFS evidence for linear two-coordination with reduced sulfur groups. Environ Sci Technol 2006, 40, (13), 4174-80.

43. Drexel, R. T.; Haitzer, M.; Ryan, J. N.; Aiken, G. R.; Nagy, K. L., Mercury(II) sorption to two Florida Everglades peats: evidence for strong and weak binding and competition by dissolved organic matter released from the peat. Environ Sci Technol 2002, 36, (19), 4058-64.

44. Wang, R.; Wang, W. X., Importance of speciation in understanding mercury bioaccumulation in Tilapia controlled by salinity and dissolved organic matter. Environ Sci Technol 2010, 44, (20), 7964-7969.

Table 1. Proportion (%) of regulated contigs in main MapMan categories (FDR < 0.1 %) after 2h exposure of *E. nuttallii* to a range of IHg and MeHg concentrations.

	IHg (µg·L^{-1})			MeHg (µg·L^{-1})			
Category	**0.015**	**0.15**	**15**	**0.01**	**0.1**	**1**	**10**
amino acid metabolism	0.5	2.6	3.1	2.1	1.9	1.3	1.4
cell structure	6.5	8.5	10.3	8.4	8.6	7.1	7.4
energy metabolism	5.7	10.3	11.6	7.1	6.8	5.0	5.4
gene regulation	21.2	25.6	22.9	28.0	30.0	29.0	28.4
other	3.5	8.6	8.4	6.7	6.9	6.6	7.7
redox	0.9	1.2	1.4	1.4	1.2	1.1	1.2
secondary metabolism	1.0	4.2	2.7	2.3	2.3	1.4	1.7
stress	2.0	3.7	3.0	3.0	3. 5	2.5	2.1
transport	2.3	8.7	8.2	4.6	5.4	3.5	3.8
unknown	56.3	26.4	28.1	35.9	33.1	42.4	40.9

Table 2. Proportion (%) of contigs regulated (FDR < 0.1 %) after 2h exposure of *E. nuttallii* to increasing IHg and MeHg concentrations in various transporter categories. Color intensity increases with increasing numbers.

Transporters	IHg (µg·L^{-1})						MeHg (µg·L^{-1})							
	0.015		0.15		15		0.01		0.1		1		10	
	up	down	up	down	up	down	up	down	up	down	up	down	up	down
nitrate				35.3		0.0		23.5		47.1		26.5	2.9	5.9
ammonium		4.0		28.0		12.0		28.0		28.0		24.0	4.0	8.0
metabolite transporters at the envelope membrane	1.7	2.3		9.3		5.8	2.3	9.9	2.9	11.6	16.9	19.8	16.9	12.8
metabolite transporters at the mitochondrial membrane	1.4		0.3	1.4		1.4	3.3	1.9	1.4	2.5	9.3	4.4	13.7	3.3
ABC transporters and multidrug resistance systems		0.8	0.2	7.0		3.1	0.5	5.9		10.3	1.7	15.9	3.9	7.3
p- and v-ATPases	2.3	1.5		8.8		4.4	2.6	10.8	1.2	13.5	17.3	17.3	21.3	3.8
H+ transporting pyrophosphatase							2.7			2.7	10.8		51.4	
calcium	3.0			0.7			0.7	1.5		2.2	11.9	3.0	13.4	0.7
potassium		1.0		3.0		3.0	0.5	2.5	1.5	5.6	4.1	9.6	5.6	3.6
anions			1.1	0.0	1.1	0.0	2.1		3.2	1.1	2.1		12.6	
cations	1.4		0.5	1.9		1.4	2.4	4.3	3.3	2.9	14.4	5.3	18.2	3.3
misc	0.3	0.5	0.5	1.8		1.3	1.8	3.6	0.3	5.1	6.3	8.1	7.1	7.6
amino acids			1.0	1.9		1.4		6.3	1.0	3.4	2.4	6.8	3.9	9.2
peptides and oligopeptides			0.6				0.6	1.2		1.2	1.2	15.7	1.2	18.6
phosphate				5.4		2.7		1.4		8.1		16.2	6.8	8.1
sugars				2.2		1.3		2.2	0.4	2.2	11.9	7.9	19.4	5.7
proteins				1.0		1.0		8.0	5.0	1.0	11.0	19.0	7.0	31.0
sulphate				8.7						4.3		19.6	2.2	8.7
metal				3.1		1.2		1.6		4.7	5.1	7.8	9.0	6.3
porins									2.9		28.6	2.9	31.4	2.9
nucleotides									3.0		6.1	4.5	1.5	6.1
cyclic nucleotide or calcium regulated channels										2.9		5.7	5.7	5.7
auxin (hormone)											2.2		4.3	17.4
peroxisomes											10.0			
arsenite-transporting ATPase													22.2	

Table 3. Chlorophyll content, anthocyanin content and activities of anti-oxidative stress enzymes (POD, class III peroxidases; SOD, superoxide dismutases) in *E. nuttallii* exposed 2h to IHg or MeHg (results are presented as % of control; bold characters indicate significant difference with *control*, mean ± SD, n = 3; t-test *p*-value < 0.05).

Treatment ($\mu g \cdot L^{-1}$)		chlorophyll (%)	anthocyanin (%)	POD activity (%)	SOD activity (%)
IHg	*control*	100.0 ± 15.2	-	100 ± 67.9	100 ± 8.5
	0.015	77.3 ± 16.2		156.2 ± 54.4	117.1 ± 24.8
	0.15	**70.5 ± 9.6**		264.0 ± 8.5	**167.9 ± 27.4**
	15	**66.7 ± 9.9**		20.8 ± 10.7	84.26 ± 12.6
MeHg	*control*	100.0 ± 18.7	100.0 ± 10.3	100.0 ± 20.62	100 ± 8.9
	0.01	82.4 ± 35.3	**764.2 ± 103.2**	280.0 ± 132.5	86.3 ± 9.0
	0.1	91.8 ± 21.3	502.5 ± 227.9	**328.0 ± 69.5**	87.0 ± 5.9
	1	96.0 ± 5.7	315.2 ± 89.0	**240.9 ± 56.4**	66.8 ± 22.4
	10	113.0 ± 11.7	**483.7 ± 108.1**	151.6 ± 33.1	94.0 ± 5.9

Supporting information

RNA-Seq

Libraries of cDNA were prepared using the TruSeq mRNA stranded kit following manufacturer's instructions and sequenced on Illumina HiSeq 2000 (Illumina, San Diego, CA, USA) with 0.5-1 µg as total RNA input. *De novo* assembling of the transcriptome was realized using Oases (0.2.08; http://www.ebi.ac.uk/~zerbino/oases/). We obtained 181'663 contigs on which reads were mapped using MAQ (0.7.1). Differential gene expression (DGE) was analyzed in CLC Main Workbench (7.7.1, https://www.qiagenbioinformatics.com/) on the 99'030 contigs that had a minimum coverage of 20 reads in at least one sample. Counts were normalized by contig length and library size. DGE were computed with the EdgeR Bioconductor package, generating fold change (FC) and false discovery rate corrected p-values (FDR). We defined significantly differently expressed contigs at a threshold of FDR <0.1% (Table S1). Reads and raw data were submitted to NCBI public database (PRJEB6266) and EMBL ArrayExpress archive (E-MTAB-2557).

Effects of IHg and MeHg on chlorophyll, anthocyanin and anti-oxidative stress enzyme

Chlorophyll and anthocyanin contents were assessed by spectrophotometry as described in detail elsewhere [1]. Briefly, for chlorophyll, after extraction in 80 % acetone in the dark, absorbance of the extract was measured at 663 and 647 nm and µg of chlorophyll calculated using the formula: $(DO_{663nm} \times 7.15) + (DO_{647nm} \times 18.71)$. For anthocyanin, after extraction in 1 % methanol-HCl, absorbance of the extract was measured at 530 and 657 nm and µg of anthocyanin calculated using the formula: $DO_{530nm} - (DO_{657nm} \times 0.25)$.

The activities of class III peroxidases (POD) and superoxide dismutases (SOD) were measured as described in detail elsewhere [2]. Briefly, 20-50 mg of frozen ground plants were homogenized in 0.3 mL buffer containing 7.76 $g \cdot L^{-1}$ potassium phosphate, 584 $mg \cdot L^{-1}$ EDTA, 391 $mg \cdot L^{-1}$ mercaptoethanol and 0.5% Triton X-100. After centrifugation (10 min, 13'000*g*, 4°

C), the supernatant was isolated and the activity of SOD and POD were measured by spectrophotometry.

Mercury analysis

Total Hg (THg = MeHg + IHg) concentration in lyophilized shoots were measured using an Advanced Hg Analyzer AMA 254 (Altec s.r.l., Czech Republic). Detection limit defined as 3× the standard deviation (s.d.) of 10 blank measurements was 0.05 ng_{THg}. The accuracy of the measurements was checked by analyzing the certified reference material (CRM) Mess-3 and TORT-2. Recovery was respectively of 100 ± 0.1% and 94.5 ± 1.1 % respectively. THg in media were measured by MERX-T [3]. Detection limit was 0.04 $ng_{THg} \cdot L^{-1}$. The accuracy of THg measurements was tested by analyzing the CRM ORMS-5 (95.0 ± 1.7 % recovery). MeHg in shoots was extracted by HNO_3 leaching, 12h at 60 °C. Shoots and media samples were then analyzed by MERX-M. Detection limit was 0.01 $ng_{MeHg} \cdot L^{-1}$. The accuracy of MeHg measurements was tested by analyzing the CRM TORT-2. Its recovery was 86.6 ± 5.2 %. IHg concentrations were calculated by subtracting MeHg content from THg content making the assumption that other forms of Hg (e.g. Hg^0) were negligible.

Chemical speciation modeling

The chemical speciation of IHg, MeHg and Cu in the exposure solutions were calculated by an iterative procedure in excel. To avoid calculation errors, the correct number on all stability constants used were confirmed by a backwards calculation from the chemical species composition in the final model. Constants in the model (Table S4) were corrected for the ionic strength in the experiments by use of the Debye-Hückel model, relevant for $I < 0.005$ M.

We used recently updated stability constants for the complexation of MeHg and Hg to natural organic matter thiol groups (NOM-RSH), as reported by Liem-Nguyen *et al.* (2017), to represent constants for the bonding of MeHg and Hg to thiol groups associated with Suwanee River HA (HA-RSH) [4]. The concentration of HA-RSH was estimated from S K-edge XANES determinations conducted at the mid-energy X-ray station, beamline 4B7A, at the Beijing Synchrotron Radiation Facilities (BSRF), China. The concentration of Org-S_{RED} (sum of RSH+RSR+RSSR [5]) groups was 66% of total S, and in agreement with Skyllberg *et al.* (2006) we estimated that RSH groups contributed 30% of Org-S_{RED}.

As compared to MeHg and Hg, there is less consensus about the thermodynamic stability of the complexation of Cu^{2+} to HA functional groups. This has to do with Cu^{2+} forming complexes with O, N and S functionalities having a quite similar strength and also the difficulty of accounting for the possible transformation of Cu^{2+} to Cu^{+} in natural and experimental systems. However, in the expected absence of significant amounts of Cu^{+}, we used the approach taken by Craven *et al.* (2012), relating the *log K* for the formation of a conditional complex CuHA-L to the CuHA-L/HA mass ratio [6]. From their reported data we derived the empirical relationship illustrated in Figure S3. The log K for the reaction Cu^{2+} + HA-L = CuHA-L was calculated by an iterative procedure, assuming [CuHA-L] = [HA-L] at equilibrium. The latter is a consequence of *log K* decreasing successively with increasing Cu/HA mass ratio. We obtained *log K* for CuHA-L values in the range 10.4 – 12.9 in our experiments. The larger constants is expected to be in the range of amino complexes and in the lower end we expect to find complexes with mainly oxygen functional groups. Stability constants for inorganic MeHg and Hg complexes were taken from Powell *et al.* (2004) [7] and for inorganic Cu(II) complexes we used generic constants from the software WHAM [8].

Since we cannot outrule the formation of Cu^{+} in our experimental systems we also performed calculations in which Cu(I) dominated over Cu(II). Cu(I) is known to form strong complexes with HA-RSH groups and could therefore compete with MeHg and Hg for thiol groups. Chapman *et al.* (2004) quantified naturally occurring NOM associated thiol ligands (L') in marine environments and reported them in glutathione equivalents [9]. Their reported *log K'* of 13.1 for CuL corresponds to 22.4 for the reaction Cu^{+} + HA-RS^{-} = CuHA-RS, if pKa of the thiol group is set similar to glutathione (9.3) [9].

Speciation modelling and uptake in presence of IHg, MeHg, Cu and SRHA

While no significant effect on $[THg]_{intra}$ uptake was observed for high IHg, high IHg + MeHg and high IHg + Cu in 0 and 1 $mg \cdot L^{-1}$ SRHA (Figure 2B), a significant decrease in $[THg]_{intra}$ uptake was observed for 10 $mg \cdot L^{-1}$ SRHA in the two latter treatments. This effect is understood from the changes in chemical speciation from a high dominance of IHg and MeHg complexed by the inorganic ligands Cl^{-} and OH^{-} to a dominance of RS groups associated with DOM at 10 $mg \cdot L^{-1}$ SRHA (Table 3). While the plant uptake after SRHA additions to treatments of IHg +

MeHg/Cu may be largely understood from chemical speciation modeling, an explanation of the results from MeHg + Cu is more demanding. The two main factors that need to be considered are: 1) the competitive effect of Cu for plant uptake of MeHg and IHg, understood as a competition for functional groups (likely RS) regulating uptake in cells; and 2) the competitive effect of Cu(II) and possibly Cu(I) with IHg and MeHg for functional groups associated with SRHA. Here, we hypothesize that inorganic forms of metals are more available for uptake than metals complexed by DOM [10, 11]. Without SRHA, all metal complexes are inorganic and the competition for plant uptake (factor 1), should drive the results. For low IHg treatments, the addition of 1 $mg \cdot L^{-1}$ and 10 $mg \cdot L^{-1}$ SRHA decreases the Hg (and MeHg) uptake *vs* 0 $mg \cdot L^{-1}$ SRHA. This can be explained mainly by a decreased fraction of inorganic complexes of Hg with addition of SRHA (Table 3). Due to the complexation by SRHA functional groups, also the competitive effect of Cu on the plant uptake decreased when SRHA was increased. However, because the relative strength in bonding between organic functional groups and inorganic ligands is smaller for Cu (as compared to IHg and MeHg), the effect on the inorganic fraction of Cu is much less pronounced. Thus the competitive effect by Cu in plant uptake persists even when SRHA increased. For high IHg treatments, there is no significant change in the inorganic fraction of either IHg, MeHg or Cu (Table 3) with 1 $mg \cdot L^{-1}$ SRHA, consistent with measured uptake (Figure 2B). The stronger effect of Cu addition at high vs low IHg, can be explained by Cu(II) maintaining a large fraction of inorganic species even at 10 $mg \cdot L^{-1}$ SRHA, which maintains factor 1, as more predominant (Table 3). However, the most striking effect of Cu addition concerns the MeHg treatments. The increased $[THg]_{intra}$ uptake in presence of SRHA + Cu suggests makes MeHg was more bioavailable with Cu. This could be understood if the competitiveness of Cu for plant uptake decreases with addition of SRHA, but our Cu(II) model shows the inorganic Cu fraction is largely unchanged at 1 $mg \cdot L^{-1}$ SRHA (Table 3). However, if Cu(I) is formed in our experiment, which is not unlikely given the

experimental conditions and uptake mechanisms of Cu as Cu(I), which is conserved through Eukaryotes including terrestrial and aquatic plants [12-14], it can be expected that Cu(I) would much more efficiently compete with MeHg for RS functional groups of SRHA. We thus made a calculation assuming all Cu added was reduced to Cu(I) and that the bonding to SRHA RS was similar in strength to RS encountered in aquatic environments [9]. Our assumption that all Cu(II) is transformed to Cu(I) is obviously an exaggeration, but in principal our calculation shows that Cu(I) would compete efficiently with MeHg with 1 $mg \cdot L^{-1}$ SRHA (Table 3) and in essence occupy all RS groups. With 10 $mg \cdot L^{-1}$ SRHA, the reduced S groups in the SRHA should be enough to bind in principal all Cu(I) and MeHg, but because of differences in the relative binding strengths, the concentration of the inorganic fraction of Cu would be substantially smaller than the inorganic fraction of MeHg. This suggests that factor 1) – the competition for plant uptake, gets in favor of MeHg at 10 $mg \cdot L^{-1}$ SRHA. Our data suggest that Cu^{2+} could be reduced to Cu^{+} in presence of SRHA in our experimental conditions. Because IHg forms relatively stronger complexes with DOM, involving two RS groups, than MeHg, Cu(I) would have a less of a competitive effect in the IHg + Cu treatments [15].

Similarly, without SRHA, Cu + IHg/MeHg significantly decreased Cu uptake. Cu uptake significantly increased when 1 $mg \cdot L^{-1}$ SRHA was added in mixtures, but not in Cu treatment only (t-test, *p*-value = 0.06; Figure S2). With 10 $mg \cdot L^{-1}$ SRHA, $[Cu]_{intra}$ was not significantly different vs without SRHA, except for Cu + MeHg, for which Cu uptake significantly decreased (1.4×), confirming the interaction between Cu and IHg/MeHg, confirming previously observed competition of Cu on $[THg]_{intra}$ uptake and increased $[THg]_{intra}$, in MeHg + Cu mixtures.

Table S1. Differential expression analysis (EdgeR log2FC and FDR and blastx annotation) of significant contigs (FDR<0.1%) after 2h inorganic Hg (0.015, 0.15 or 15 $\mu g \cdot L^{-1}$) or methyl Hg (0.01, 0.1, 1 or 10 $\mu g \cdot L^{-1}$) exposure in *Elodea nuttallii* (XLSX File).

Table S2. Description of the nCounter probes, their RNA-Seq (*experiment 1*) and nCounter results (*experiment 2*) (annotation was obtained in Blast2GO using blastx against the NCBI Viridiplantae database and MapMan ontology, n.a., not annotated) (XLSX file).

Table S3. Measured concentrations in the medium at beginning of experiment 1 and 2 (mean ± SD, n=3). The presence of SRHA had no significant effect on initial THg, MeHg or Cu water concentrations (t-test $p<0.05$).

Experiment		Treatment	$[THg]_{med}$ ($\mu g \cdot L^{-1}$)	$[MeHg]_{med}$ ($\mu g \cdot L^{-1}$)	$[Cu]_{med}$ ($\mu g \cdot L^{-1}$)
		control	*0.22 ± 0.09* ng·L^{-1}	*0.15 ± 0.06* ng·L^{-1}	*<dl*
1. RNA-Seq	IHg ($\mu g \cdot L^{-1}$)	0.015	0.02 ± 0.00		
		0.15	0.13 ± 0.02		
		15	14.39 ± 0.17		
	MeHg ($\mu g \cdot L^{-1}$)	0.01	0.01 ± 0.00	0.01 ± 0.00	
		0.1	0.09 ± 0.01	0.08 ± 0.02	
		1	0.53 ± 0.08	0.90 ± 0.02	
		10	4.32 ± 0.14	10.01 ± 0.50	
2. nCounter	single	0.15 µg·L^{-1} IHg	0.11 ± 0.01		
		15 µg·L^{-1} IHg	11.02 ± 0.09		
		0.25 µg·L^{-1} MeHg	0.12 ± 0.01	0.32 ± 0.04	
		4 µg·L^{-1} Cu			4.72 ± 0.24
	mixture	0.15 µg·L^{-1} IHg + 0.25 µg·L^{-1} MeHg	0.44 ± 0.06	0.29 ± 0.08	
		15 µg·L^{-1} IHg + 0.25 µg·L^{-1} MeHg	11.02 ± 0.09	0.29 ± 0.08	
		0.15 µg·L^{-1} IHg + 4 µg·L^{-1} Cu	0.44 ± 0.06		3.81 ± 0.02
		70 µg·L^{-1} IHg + 4 µg·L^{-1} Cu	71.58 ± 2.95		4.06 ± 0.02
		0.25 µg·L^{-1} MeHg + 17 µg·L^{-1} Cu		0.27 ± 0.03	16.94 ± 0.15

Table S4. Stability constants used in chemical speciation model.

	Log K (*I=0.65 mM*)	Ref
$Hg^{2+} + Cl^- = HgCl^+$	7.05	[7]
$Hg^{2+} + 2Cl^- = HgCl_2$	13.72	[7]
$Hg^{2+} + 3Cl^- = HgCl_3^-$	14.61	[7]
$Hg^{2+} + 4Cl^- = HgCl_4^{2-}$	15.35	[7]
$Hg^{2+} + OH^- = HgOH^+$	10.25	[7]
$Hg^{2+} + 2OH^- = HgOH_2$	21.32	[7]
$MeHg^+ + Cl^- = MeHgCl$	5.37	[7]
$MeHg^+ + OH^- = MeHgOH$	9.47	[7]
$Cu^{2+} + Cl^- = CuCl^+$	0.35	[8]
$Cu^{2+} + OH^- = CuOH^+$	6.45	[8]
$Cu^{2+} + 2OH^- = Cu(OH)_2$	11.70	[8]
$Cu^{2+} + SO_4^{2-} = CuSO_4$	2.26	[8]
$Cu^{2+} + CO_3^{2-} = CuCO_3$	6.65	[8]
$Cu^{2+} + 2CO_3^{2-} = Cu(CO_3)_2^{2-}$	9.82	[8]
$Cu^{2+} + HCO_3^- = CuHCO_3^+$	14.56	[8]
$HA\text{-}RSH = HA\text{-}RS^- + H^+$	-8.99	[4]
$Hg^{2+} + 2HA\text{-}RS^- = Hg(HA\text{-}RS)_2$	40.9	[4]
$MeHg^+ + HA\text{-}RS^- = MeHgHA\text{-}RS$	17.44	[4]
$Cu^{2+} + HA\text{-}L = CuHA\text{-}L$	-1.342 ln(Cu/HA) + 2.33	[6]

Table S5. Total Hg (THg = IHg + MeHg) and MeHg accumulated in *E. nuttallii* exposed 2 h in *experiment 1* (RNA-Seq). Number of reads, % of mapped reads on the *de novo* transcriptome and differential gene expression analysis (FDR <0.1%). Shoots exposed to IHg and MeHg were respectively washed with EDTA and EDTA + cysteine to determine intracellular Hg concentrations, or rinsed with water (unwashed) to estimate Hg concentration adsorbed on shoots' surface (dw, dry weight, n=3 ± SD). The washing procedure had no significant effect on Hg concentration in *control* (n = 6; t-test p<0.05).

Treatment ($\mu g \cdot L^{-1}$)		**$[THg]_{plant}$ ($\mu g \cdot g^{-1}$, dw)**		**$[MeHg]_{plant}$ ($\mu g \cdot g^{-1}$, dw)**		**Number of reads ($\cdot 10^6$)**	**% reads mapped**	**Number of significant differentially regulated contigs**		
		washed shoots	unwashed shoots	washed shoots	unwashed shoots			up-regulated	down-regulated	Total (% of all contigs)
IHg	***control***	*0.039 ± 0.007*		-		21.4	71.6			
	0.015	0.063 ± 0.008	0.186 ± 0.068			6.7	69.3	1296	219	1515 (1.5)
	0.15	0.359 ± 0.017	0.423 ± 0.092			11.0	69.1	359	1318	1677 (1.7)
	15	40.27 ± 7.11	56.27 ± 3.54			5.8	70.2	212	627	839 (0.8)
MeHg	***control***	*0.065 ± 0.016*		*0.022 ± 0.009*		*21.4*	*71.6*			
	0.01	0.072 ± 0.010	0.074 ± 0.003	0.037 ± 0.002	0.049 ± 0.006	6.3	69.7	2092	2306	4398 (4.4)
	0.1	0.214 ± 0.005	0.217 ± 0.020	0.148 ± 0.026	0.155 ± 0.026	13.6	69.4	1777	2818	4595 (4.6)
	1	1.538 ± 0.109	1.605 ± 0.199	0.886 ± 0.076	1.269 ± 0.100	21.3	71.0	9719	8838	18557 (18.7)
	10	18.34 ± 2.76	19.25 ± 1.59	10.93 ± 0.92	13.91 ± 0.60	23.9	73.0	7892	8961	16853 (17.0)

Table S6. Number of significant regulated contigs in the MapMan biological pathways and detailed ontology for the 7 RNA-Seq experiment treatments (XLSX File).

Table S7. Speciation modelling of IHg, MeHg and Cu in absence or presence of Suwannee River Humic Acid (XLSX File).

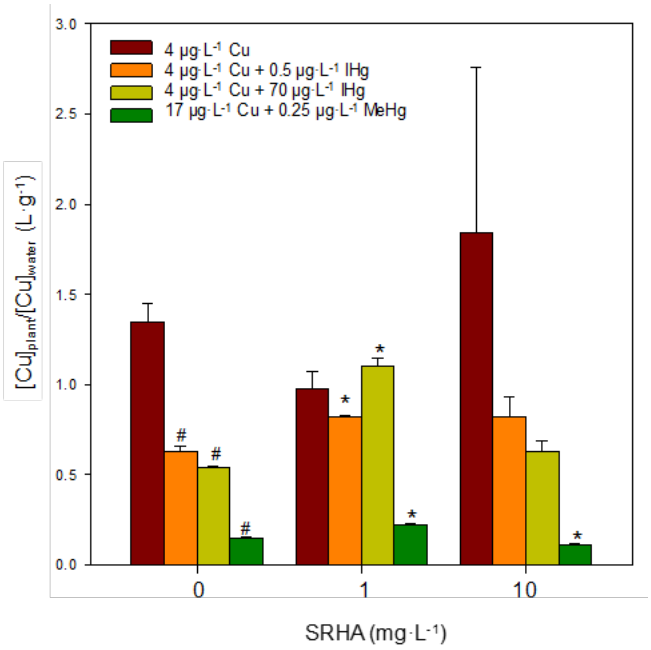

Figure S1. Cu uptake in *E. nuttallii* after 2h exposure in single and mixtures with Cu, IHg or MeHg, and SRHA. * indicate a significant effect of SRHA compared to the respective treatment without SRHA and # indicate a significant difference *vs* Cu alone in the absence of SRHA (mean ± SD, n = 2, T-test, p-value <0.01).

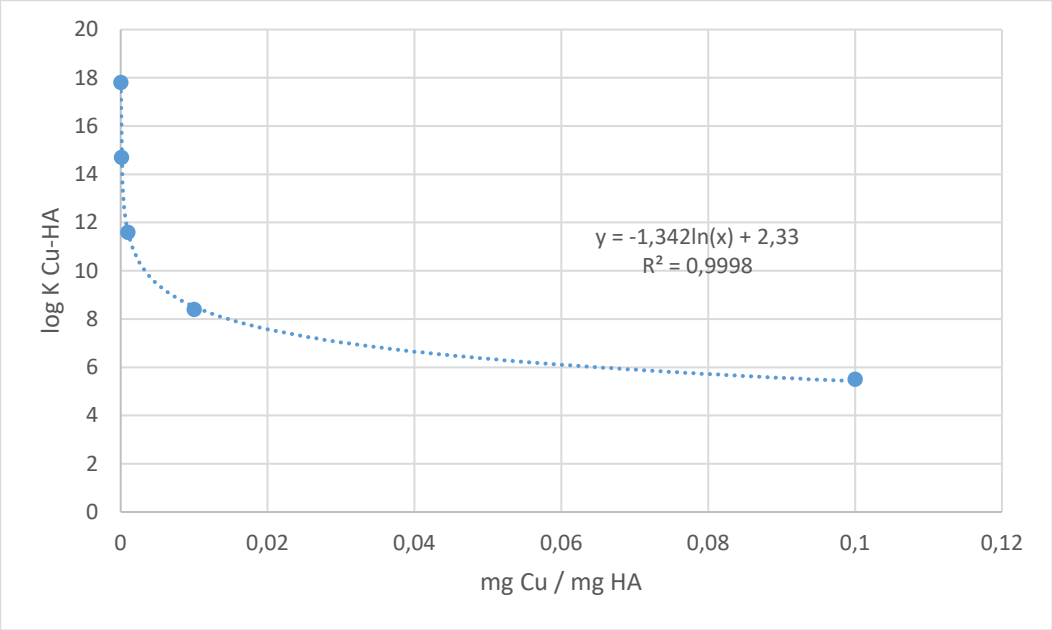

Figure S2. Relationship between Cu to HA mass ratio (in the Cu-HA-L complex) and log K for the formation of the CuHA-L complex according to Craven et al. (2012) [6].

References:

1. Cosio, C.; Dunand, C., Transcriptome analysis of various flower and silique development stages indicates a set of class III peroxidase genes potentially involved in pod shattering in *Arabidopsis thaliana*. *Bmc Genomics* **2010,** *11*, 16.
2. Regier, N.; Beauvais-Flück, R.; Slaveykova, V. I.; Cosio, C., *Elodea nuttallii* exposure to mercury exposure under enhanced ultraviolet radiation: Effects on bioaccumulation, transcriptome, pigment content and oxidative stress. *Aquat Toxicol* **2016,** *180*, 218-226.
3. USEPA, Method 1631: Mercury in water by oxidation, purge and trap, and CVAFS. *USEPA, Office of Water,* **2002**.
4. Liem-Nguyen, V.; Skyllberg, U.; Bjorn, E., Thermodynamic modeling of the solubility and chemical speciation of mercury and methylmercury driven by organic thiols and micromolar sulfide concentrations in boreal wetland soils. *Environ Sci Technol* **2017,** *51*, (7), 3678-3686.
5. Skyllberg, U.; Bloom, P. R.; Qian, J.; Lin, C. M.; Bleam, W. F., Complexation of mercury(II) in soil organic matter: EXAFS evidence for linear two-coordination with reduced sulfur groups. *Environ Sci Technol* **2006,** *40*, (13), 4174-80.
6. Craven, A. M.; Aiken, G. R.; Ryan, J. N., Copper(II) binding by dissolved organic matter: importance of the copper-to-dissolved organic matter ratio and implications for the biotic ligand model. *Environ Sci Technol* **2012,** *46*, (18), 9948-9955.
7. Powell, K. J.; Brown, P. L.; Byrne, R. H.; Gajda, T.; Hefter, G.; Sjöberg, S.; Wanner, H., Chemical speciation of Hg(II) with environmental inorganic ligands. *Aust J Chem* **2004,** *57*, (10), 993-1000.
8. Tipping, E.; Lofts, S., Testing WHAM-FTOX with laboratory toxicity data for mixtures of metals (Cu, Zn, Cd, Ag, Pb). *Environ Toxicol Chem* **2015,** *34*, (4), 788-98.
9. Chapman, C. S.; Capodaglio, G.; Turetta, C.; van den Berg, C. M., Benthic fluxes of copper, complexing ligands and thiol compounds in shallow lagoon waters. *Mar Environ Res* **2009,** *67*, (1), 17-24.
10. Paquin, P. R.; Gorsuch, J. W.; Apte, S.; Batley, G. E.; Bowles, K. C.; Campbell, P. G. C.; Delos, C. G.; Di Toro, D. M.; Dwyer, R. L.; Galvez, F.; Gensemer, R. W.; Goss, G. G.; Hogstrand, C.; Janssen, C. R.; McGeer, J. C.; Naddy, R. B.; Playle, R. C.; Santore, R. C.; Schneider, U.; Stubblefield, W. A.; Wood, C. M.; Wu, K. B., The biotic ligand model: a historical overview. *Comparative Biochem Physiol Part C: Toxicol Pharmacol* **2002,** *133*, (1), 3-35.
11. Gorski, P. R.; Armstrong, D. E.; Hurley, J. P.; Shafer, M. M., Speciation of aqueous methylmercury influences uptake by a freshwater alga (*Selenastrum capricornutum*). *Environ Toxicol Chem* **2006,** *25*, (2), 534-40.
12. Balamurugan, K.; Schaffner, W., Copper homeostasis in eukaryotes: Teetering on a tightrope. *Biochimica et Biophysica Acta (BBA) - Molec Cell Res* **2006,** *1763*, (7), 737-746.
13. Regier, N.; Larras, F.; Bravo, A. G.; Ungureanu, V. G.; Amouroux, D.; Cosio, C., Mercury bioaccumulation in the aquatic plant *Elodea nuttallii* in the field and in microcosm: accumulation in shoots from the water might involve copper transporters. *Chemosphere* **2013,** *90*, (2), 595-602.
14. Sancenón, V.; Puig, S.; Mira, H.; Thiele, D.; Peñarrubia, L., Identification of a copper transporter family in *Arabidopsis thaliana*. *Plant Mol Biol* **2003,** *51*, (4), 577-587.
15. Skyllberg, U., Competition among thiols and inorganic sulfides and polysulfides for Hg and MeHg in wetland soils and sediments under suboxic conditions: Illumination of controversies and implications for MeHg net production. *J Geophysical Res: Biogeosci* 2008, 113, (G2).